PNAS

Supplementary Information for

Body size predicts the rate of contemporary morphological change in birds

Marketa Zimova[1,2], Brian C. Weeks[2*], David E. Willard[3], Sean T. Giery[4], Vitek Jirinec[5,6], Ryan C. Burner[7], and Benjamin M. Winger[8,*]

[1] Department of Biology, Appalachian State University, 572 Rivers Street, Boone, NC 28608, USA.[2] School for Environment and Sustainability, University of Michigan, 440 Church St, Ann Arbor, MI 49109, USA. [3] Gantz Family Collection Center, The Field Museum, 1400 S. Lake Shore Dr., Chicago, IL 60605, USA. [4] Department of Biology, The Pennsylvania State University, University Park, PA 16802, USA. [5] Integral Ecology Research Center, 239 Railroad Ave, Blue Lake, CA 95525, USA. [6] School of Renewable Natural Resources, Louisiana State University and LSU AgCenter, Baton Rouge, LA 70803, USA. [7] U.S. Geological Survey, Upper Midwest Environmental Sciences Center, 2630 Fanta Reed Road, La Crosse, WI, 54603, USA. [8] Museum of Zoology and Department of Ecology and Evolutionary Biology, University of Michigan, 1105 N. University Avenue, Ann Arbor, MI 48109, USA.

Brian C. Weeks
Email: bcweeks@umich.edu

Benjamin M. Winger
Email: wingerb@umich.edu

This PDF file includes:

Any use of trade, firm, or product names is for descriptive purposes only and does not imply endorsement by the U.S. Government.

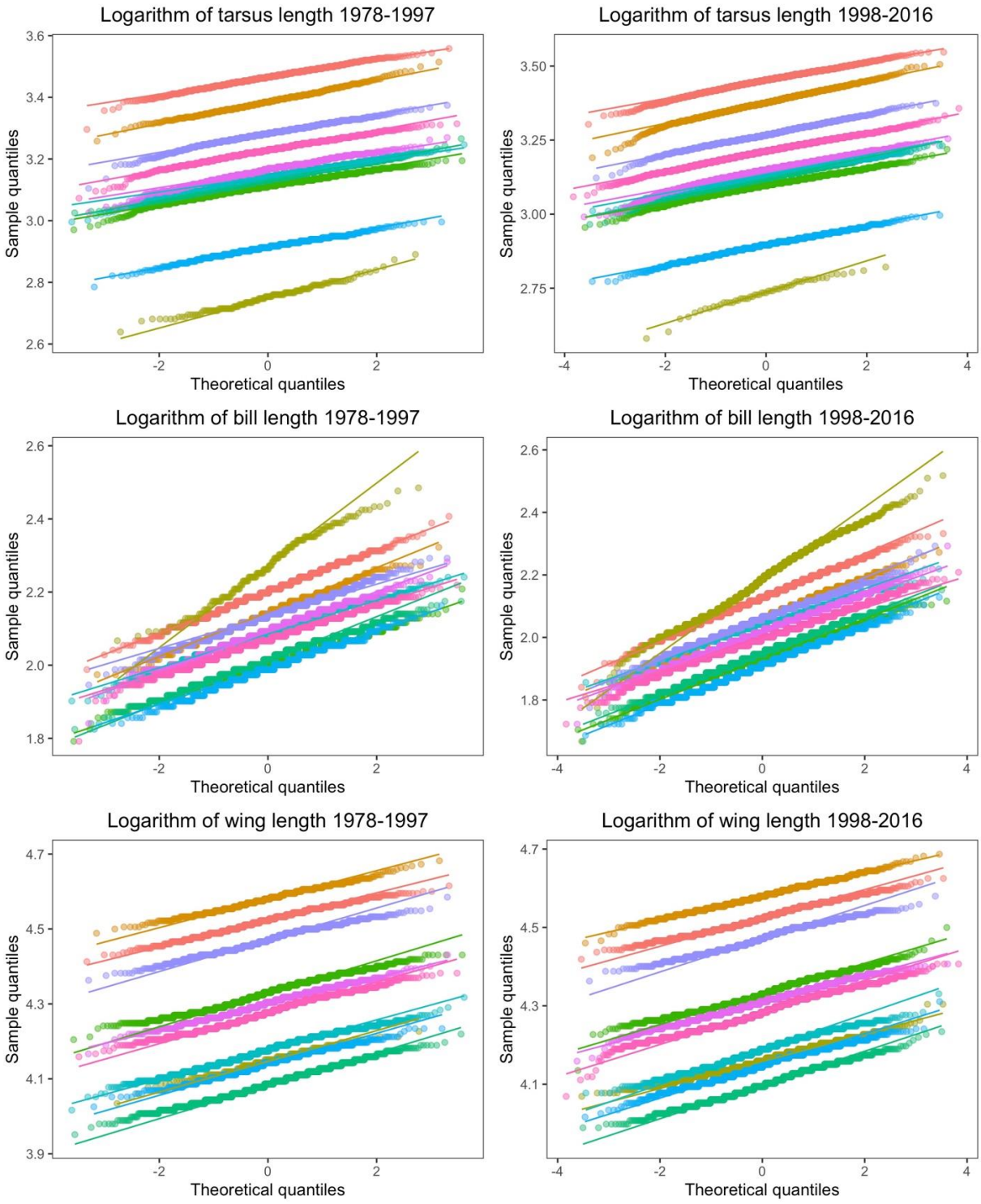

Figure S1. Quantile-quantile plots of the logarithm of each morphological trait for 10 most highly sampled species in the Chicago dataset. The first and second half of the data are shown in the left, and right panels, respectively. Different species are indicated by different colors.

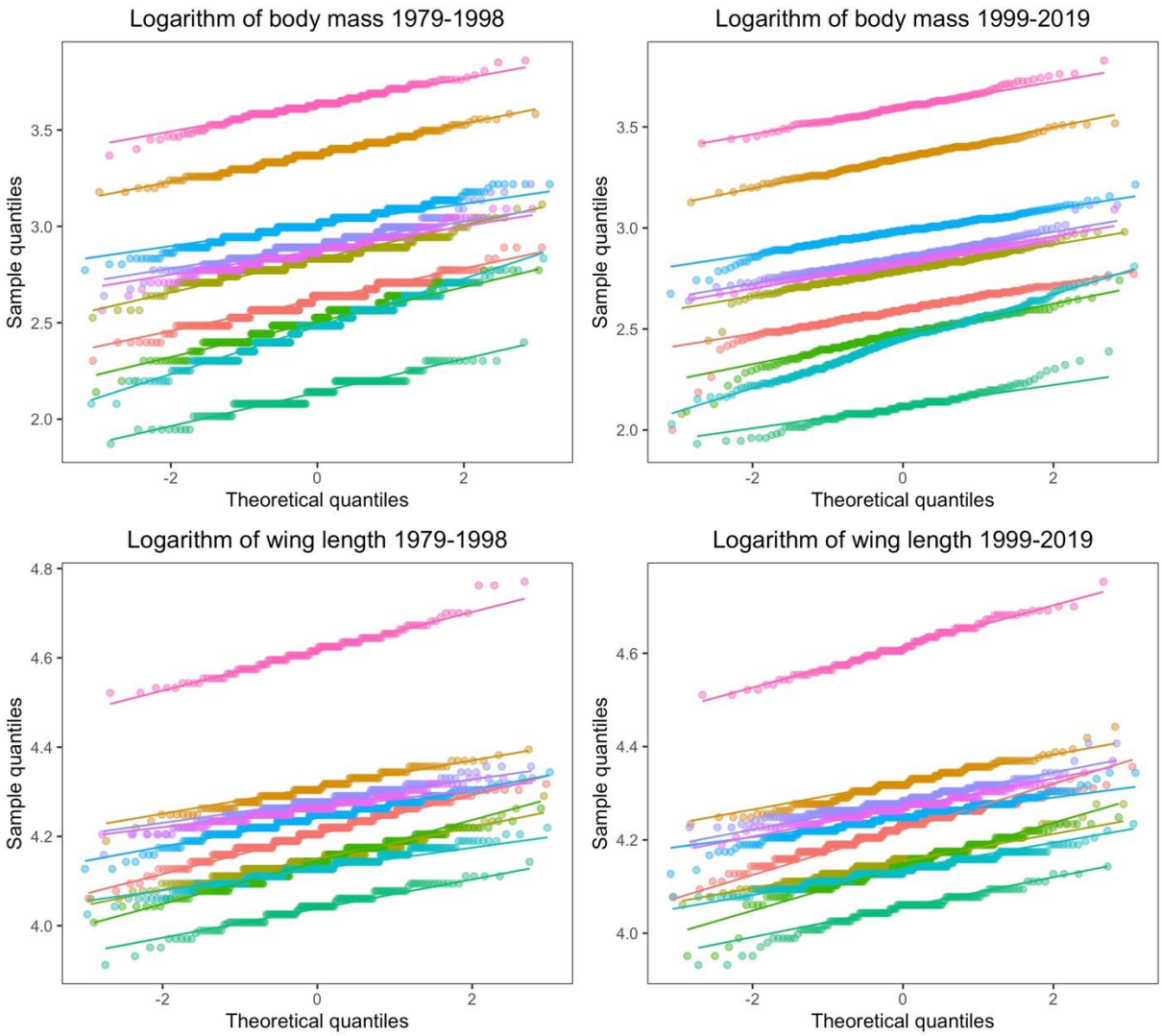

Figure S2. Quantile-quantile plots of the logarithm of each morphological trait for the most highly sampled species in the Amazon dataset. The first and second half of the data are shown in the left, and right panels, respectively. Different species are indicated by different colors.

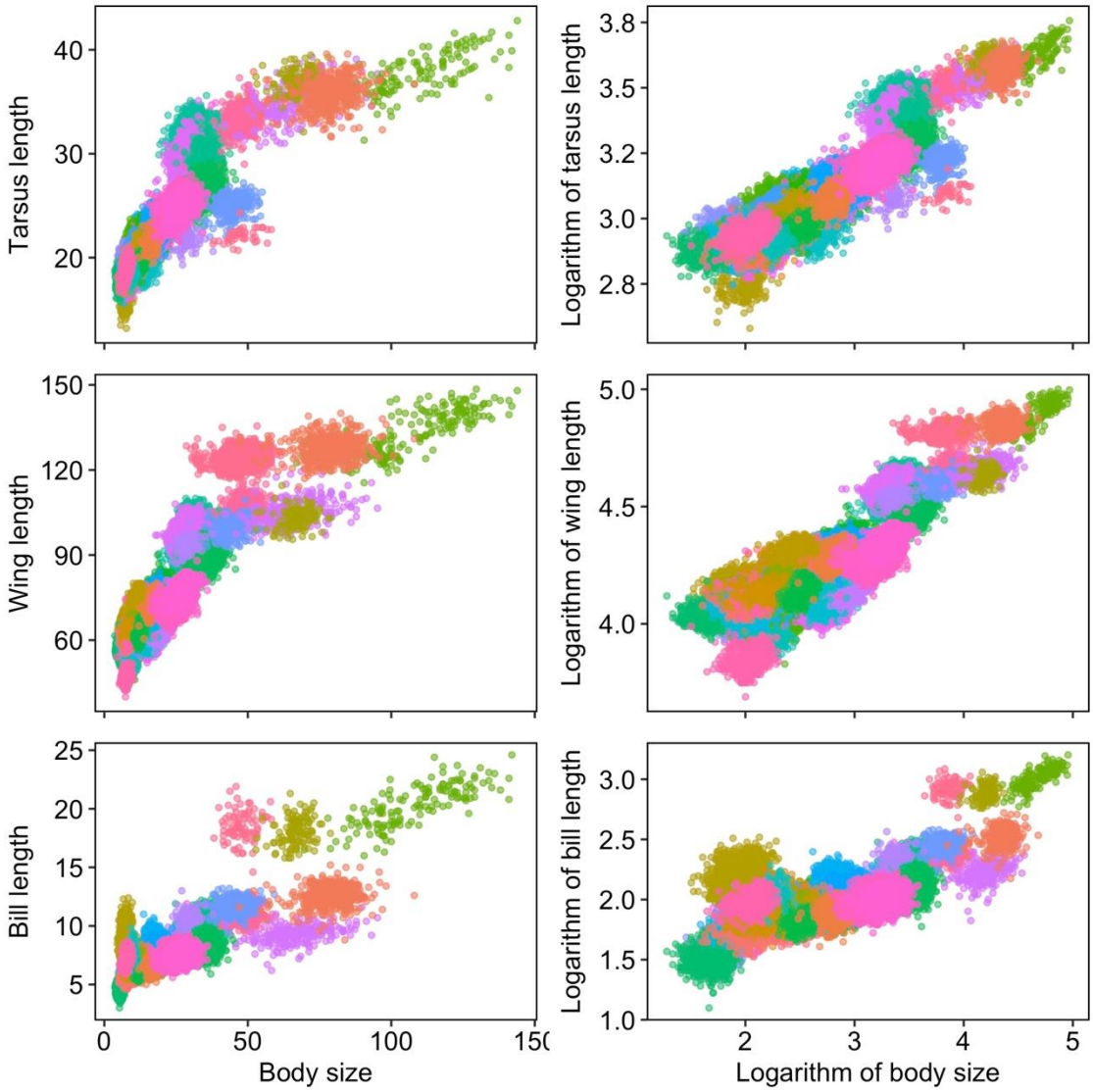

Figure S3. The relationships between body size and tarsus, wing, and bill lengths are linear on a log-log scale. Left panels show the relationships between raw data for the Chicago species, with each dot representing an individual specimen and different colors representing species. On this non-transformed scale, body size has non-linear allometric relationships with the length measurements (tarsus, wing, and bill lengths), as is expected based on geometry (1); these patterns generally conform to a 1/3 power law (*Appendix SI*, Methods S2). Right panels demonstrate that, as expected, these relationships become linear when the data are log-transformed.

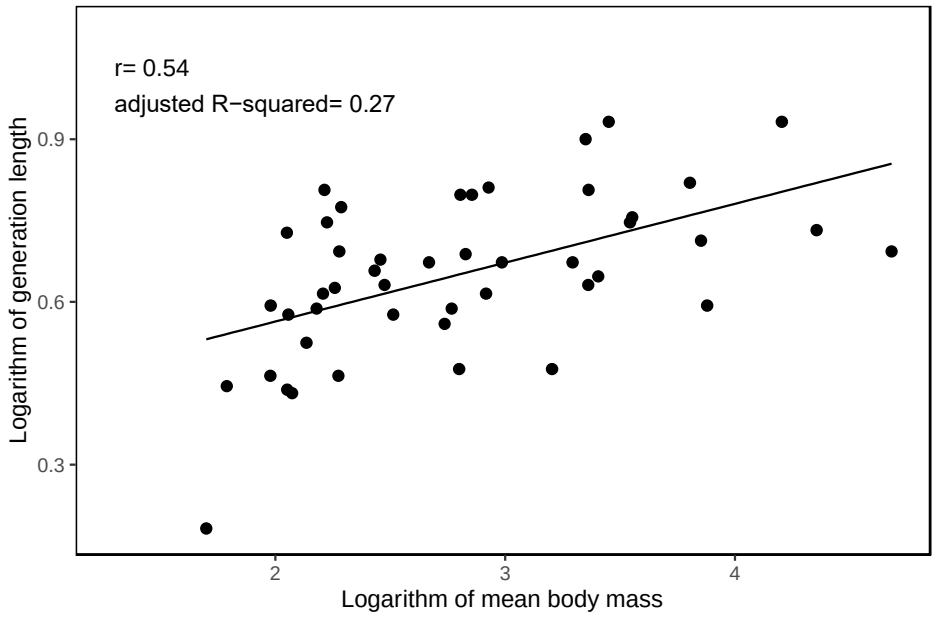

Figure S4. The logarithm of species' mean body size and the logarithm of generation length in the Chicago dataset are positively and linearly correlated, but this correlation is relatively low. The Pearson's correlation coefficient r and adjusted R^2 based on simple linear regression for all species are given in the upper left corner.

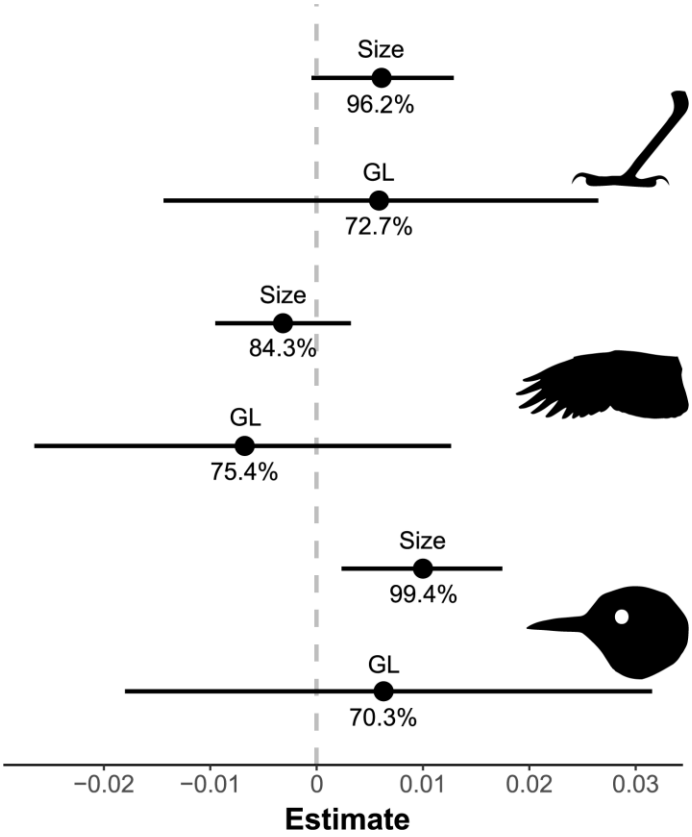

Figure S5. Estimates of the correlations between time trends in tarsus, wing, and bill lengths, and species' mean body size (Size) and generation length (GL) for 46 species from the Chicago dataset. Estimates are based on Bayesian hierarchical multi-species models that include all trait observations. All models also included sex and age covariates, and a phylogeny. Dots show median estimates, bars show 95% Bayesian credible intervals (CIs), and numbers show one-sided % posterior support values.

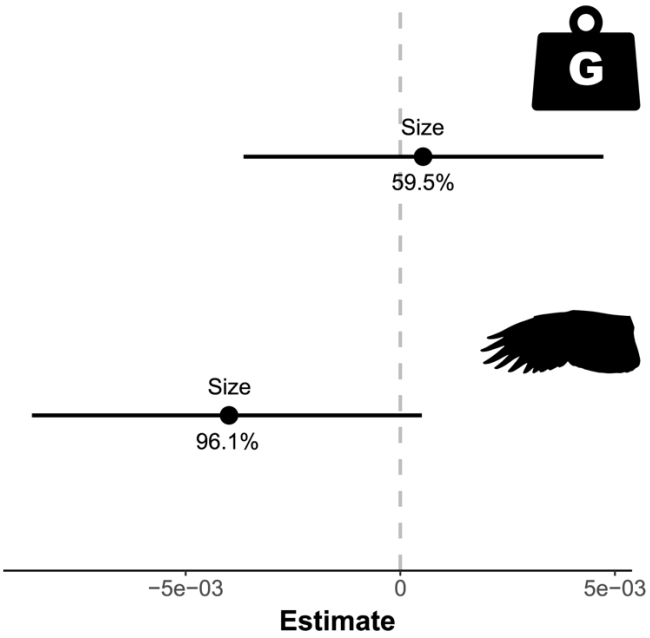

Figure S6. Estimates of the correlations between time trends in body mass and wing length, and species' mean body size (Size) for 77 species from the Amazon dataset. Estimates are based on Bayesian hierarchical multi-species models that include all trait observations and phylogeny. Dots show median estimates, bars show 95% Bayesian credible intervals (CIs), and numbers show one-sided % posterior support values.

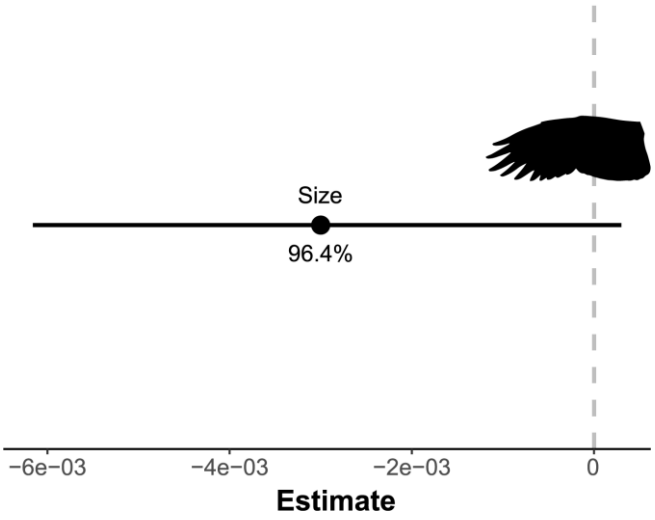

Figure S7. Estimate of the correlation between time trend in wing length and species' mean body size (Size) for 123 bird species (52 from the Chicago dataset and 77 from the Amazon dataset). Estimate is based on Bayesian hierarchical multi-species models that include all trait observations and a phylogeny. Dot shows median estimate, bars show 95% Bayesian credible intervals (CIs), and number shows the one-sided % posterior support value.

Table S1. Taxonomic sampling in the Chicago (North American) dataset (https://doi.org/10.5061/dryad.8pk0p2nhw). The dataset included 70,716 specimens from 52 species. Mean mass is species' mean body mass (g) estimated from this dataset, generation length is based on observed vital rates provided in (2), and n is sample size for each species. Taxonomy follows (3).

Family	**Scientific name**	**Mean mass**	**Generation Length**	**n**
Cardinalidae	*Passerina cyanea*	14.42	1.96	711
Cardinalidae	*Pheucticus ludovicianus*	44.88	2.27	377
Cardinalidae	*Piranga olivacea*	28.87	2.24	119
Certhiidae	*Certhia americana*	7.23	1.59	2,607
Icteridae	*Quiscalus quiscula*	107.90	2.00	227
Mimidae	*Dumetella carolinensis*	34.92	2.13	582
Mimidae	*Toxostoma rufum*	66.94	2.54	153
Parulidae	*Cardellina canadensis*	9.57	1.87	250
Parulidae	*Cardellina pusilla*	7.24	1.81	181
Parulidae	*Geothlypis philadelphia*	11.67	1.97	427
Parulidae	*Geothlypis trichas*	9.76	2.00	1,569
Parulidae	*Mniotilta varia*	9.84	2.17	618
Parulidae	*Oporornis agilis*	13.35	NA	361
Parulidae	*Leiothlypis celata*	8.84	1.80	232
Parulidae	*Leiothlypis peregrina*	9.01	NA	2,649
Parulidae	*Leiothlypis ruficapilla*	7.95	1.54	1,665
Parulidae	*Parkesia noveboracensis*	16.53	2.22	928
Parulidae	*Seiurus aurocapilla*	18.69	2.25	4,518
Parulidae	*Setophaga caerulescens*	9.25	2.11	183
Parulidae	*Setophaga castanea*	11.41	NA	282
Parulidae	*Setophaga coronata*	11.88	1.88	892
Parulidae	*Setophaga fusca*	9.15	2.24	199
Parulidae	*Setophaga magnolia*	7.82	1.78	1,220
Parulidae	*Setophaga palmarum*	9.73	NA	680
Parulidae	*Setophaga pensylvanica*	9.09	1.85	296
Parulidae	*Setophaga ruticilla*	7.77	2.07	853
Parulidae	*Setophaga striata*	11.38	1.93	791

Parulidae	*Setophaga tigrina*	9.88	NA	183
Parulidae	*Setophaga virens*	8.46	1.69	215
Passerellidae	*Ammodramus savannarum*	16.44	1.61	103
Passerellidae	*Junco hyemalis*	18.48	1.85	6,164
Passerellidae	*Melospiza georgiana*	15.43	1.75	4,897
Passerellidae	*Melospiza lincolnii*	15.91	1.80	1,986
Passerellidae	*Melospiza melodia*	19.80	1.96	5,070
Passerellidae	*Passerculus sandwichensis*	17.38	2.22	277
Passerellidae	*Passerella iliaca*	34.58	2.11	2,433
Passerellidae	*Spizella pusilla*	12.34	1.78	320
Passerellidae	*Spizelloides arborea*	16.91	1.99	1,247
Passerellidae	*Zonotrichia albicollis*	24.63	1.61	9,953
Passerellidae	*Zonotrichia leucophrys*	26.93	1.96	1,107
Picidae	*Sphyrapicus varius*	47.09	2.04	2,057
Rallidae	*Porzana carolina*	67.1	NA	380
Regulidae	*Corthylio calendula*	5.98	1.56	412
Regulidae	*Regulus satrapa*	5.47	1.20	1,020
Troglodytidae	*Troglodytes aedon*	9.72	1.59	101
Troglodytidae	*Troglodytes hiemalis*	7.78	1.55	449
Turdidae	*Catharus fuscescens*	31.52	2.54	744
Turdidae	*Catharus guttatus*	28.83	1.88	3,662
Turdidae	*Catharus minimus*	30.11	1.91	849
Turdidae	*Catharus ustulatus*	28.51	2.46	2,485
Turdidae	*Hylocichla mustelina*	48.37	1.81	462
Turdidae	*Turdus migratorius*	77.89	2.08	570

Table S2. Taxonomic sampling in the Amazonian (Brazil) dataset (https://doi.org/10.5061/dryad.fqz612jsp). The dataset included 15,415 specimens from 77 species. Mean mass is species' mean body mass (g) estimated from this dataset and n is sample size for each species. Taxonomy follows (4).

Family	**Scientific name**	**Mean mass**	**n**
Bucconidae	*Bucco capensis*	51.02	22
Bucconidae	*Malacoptila fusca*	43.65	119
Cardinalidae	*Cyanoloxia rothschildii*	25.37	63
Conopophagidae	*Conopophaga aurita*	23.24	69
Cotingidae	*Lipaugus vociferans*	69.73	24
Formicariidae	*Formicarius analis*	61.85	101
Formicariidae	*Formicarius colma*	45.81	265
Furnariidae	*Automolus infuscatus*	31.48	248
Furnariidae	*Automolus ochrolaemus*	34.09	38
Furnariidae	*Clibanornis rubiginosus*	36.50	82
Furnariidae	*Campylorhamphus procurvoides*	34.50	35
Furnariidae	*Deconychura longicauda*	27.76	60
Furnariidae	*Certhiasomus stictolaemus*	16.72	207
Furnariidae	*Dendrocincla fuliginosa*	40.25	137
Furnariidae	*Dendrocincla merula*	53.01	288
Furnariidae	*Dendrocolaptes certhia*	67.06	57
Furnariidae	*Glyphorynchus spirurus*	13.54	954
Furnariidae	*Hylexetastes perrotii*	112.51	49
Furnariidae	*Philydor erythrocercum*	23.66	90
Furnariidae	*Philydor pyrrhodes*	29.42	30
Furnariidae	*Sclerurus caudacutus*	39.12	71
Furnariidae	*Sclerurus obscurior*	25.21	48
Furnariidae	*Sclerurus rufigularis*	20.91	154

Furnariidae	*Synallaxis rutilans*	16.73	31
Furnariidae	*Xenops minutus*	12.16	151
Furnariidae	*Xiphorhynchus pardalotus*	37.38	363
Galbulidae	*Galbula albirostris*	17.80	173
Grallariidae	*Grallaria varia*	123.28	13
Grallariidae	*Hylopezus macularius*	42.07	32
Momotidae	*Momotus momota*	131.00	88
Parulidae	*Myiothlypis rivularis*	13.02	24
Pipridae	*Corapipo gutturalis*	7.92	195
Pipridae	*Ceratopipra erythrocephala*	11.80	91
Pipridae	*Pseudopipra pipra*	11.77	992
Pipridae	*Lepidothrix serena*	10.47	260
Polioptilidae	*Microbates collaris*	10.72	282
Thamnophilidae	*Frederickena viridis*	67.12	64
Thamnophilidae	*Gymnopithys rufigula*	28.98	567
Thamnophilidae	*Hylophylax naevius*	12.37	45
Thamnophilidae	*Willisornis poecilinotus*	16.68	797
Thamnophilidae	*Hypocnemis cantator*	11.79	289
Thamnophilidae	*Myrmoderus ferrugineus*	24.29	150
Thamnophilidae	*Myrmornis torquata*	43.82	102
Thamnophilidae	*Myrmotherula axillaris*	7.65	171
Thamnophilidae	*Isleria guttata*	10.24	112
Thamnophilidae	*Epinecrophylla gutturalis*	8.71	303
Thamnophilidae	*Myrmotherula longipennis*	8.42	388
Thamnophilidae	*Myrmotherula menetriesii*	8.15	223
Thamnophilidae	*Myrmelastes leucostigma*	24.23	81
Thamnophilidae	*Percnostola rufifrons*	28.55	296
Thamnophilidae	*Pithys albifrons*	20.13	1203
Thamnophilidae	*Thamnomanes ardesiacus*	17.97	521

Thamnophilidae	*Thamnomanes caesius*	17.42	521
Thamnophilidae	*Thamnophilus murinus*	17.64	102
Thraupidae	*Lanio fulvus*	25.67	29
Thraupidae	*Tachyphonus surinamus*	20.36	176
Tityridae	*Myiobius barbatus*	10.47	306
Tityridae	*Onychorhynchus coronatus*	14.46	48
Tityridae	*Schiffornis olivacea*	33.80	250
Tityridae	*Terenotriccus erythrurus*	6.71	67
Trochilidae	*Campylopterus largipennis*	8.71	47
Trochilidae	*Phaethornis bourcieri*	4.09	136
Trochilidae	*Phaethornis superciliosus*	5.50	167
Trochilidae	*Thalurania furcata*	4.08	134
Troglodytidae	*Cyphorhinus arada*	20.08	185
Troglodytidae	*Microcerculus bambla*	16.58	77
Trogonidae	*Trogon rufus*	50.52	28
Turdidae	*Turdus albicollis*	48.84	343
Tyrannidae	*Attila spadiceus*	32.63	27
Tyrannidae	*Corythopis torquatus*	14.68	173
Tyrannidae	*Mionectes macconnelli*	12.23	664
Tyrannidae	*Platyrinchus coronatus*	8.57	229
Tyrannidae	*Platyrinchus platyrhynchos*	11.92	22
Tyrannidae	*Platyrinchus saturatus*	10.34	158
Tyrannidae	*Rhynchocyclus olivaceus*	19.30	49
Tyrannidae	*Rhytipterna simplex*	33.43	25
Vireonidae	*Tunchiornis ochraceiceps*	10.06	234

Table S3. Species explained far more variance than year in a model with logarithm of mass as dependent variable and species and year as independent variables. ΔR^2s (squared semi-partial correlation coefficients) were estimated using (5).

Dataset	Variable	ΔR^2
Chicago	Species	0.9684
Chicago	Year	0.0002
Amazon	Species	0.9782
Amazon	Year	0.0005

Table S4. Relationship between rates of change in morphological traits and generation length and species' mean body size. For the Chicago dataset (Chi), rates of change in tarsus, bill, and wing lengths were modeled as a function of log-transformed estimates of species generation length (Gen. length) and mean body size (Body size). For the Amazon dataset (Ama), rates of change in body mass and wing length were modeled as a function of log-transformed estimates of mean body size (Body size). Finally, rates of change in wing length of the Chicago and the Amazon datasets combined were modeled as a function of log-transformed estimates of mean body size (Body size). All models were run with simultaneous estimation of Pagels' λ (Lambda).

Trait	Dataset	Variable	Coefficient	Standard Error	T-Value	P-Value	Lambda (95% CI)
Tarsus length	Chi	Intercept	-1.11E-03	1.28E-04	-8.989	<0.0001	0.93
		Gen. length	3.65E-05	1.01E-04	0.361	0.720	(0.74, 1.11)
		Body size	1.81E-04	2.86E-05	6.327	<0.0001	
Bill length	Chi	Intercept	-5.63E-03	7.87E-04	-7.151	<0.0001	0.94
		Gen. length	3.66E-04	5.87E-04	0.622	0.537	(0.75, 1.13)
		Body size	9.12E-04	1.72E-04	5.294	<0.0001	
Wing length	Chi	Intercept	6.16E-04	2.22E-04	2.774	0.008	0.83
		Gen. length	-1.84E-04	2.09E-04	-0.879	0.384	(0.58, 1.08)
		Body size	-1.08E-04	5.43E-05	-1.990	0.053	
Body mass	Ama	Intercept	-1.76E-03	1.01E-04	-17.408	<0.0001	0.06
		Body size	2.51E-04	3.17E-05	7.910	<0.0001	(-0.16, 0.27)
Wing length	Ama	Intercept	6.42E-04	8.58E-05	7.484	<0.0001	0.53
		Body size	-1.44E-04	2.30E-05	-6.263	<0.0001	(0.18, 0.88)
Wing length	Chi & Ama	Intercept	6.25E-04	9.58E-05	6.524	<0.0001	0.68
		Body size	-1.37E-04	2.23E-05	-6.147	<0.0001	(0.46, 0.89)

Table S5. Comparison of models testing the effects of species' mean body size and generation length (Gen. length) on rates of change in tarsus, bill, and wing lengths. Models were fit using PGLS with maximum likelihood. Int is the model intercept, K is the number of estimated parameters, logLik is log likelihood, AIC is Akaike's Information Criterion, ΔAIC is the difference in AIC value between a model and the best-fitting model in the set. Mean body size and generation length were log-transformed.

Tarsus length rate

Model	K	logLik	AIC	ΔAIC
Int + Gen. length + Body size	4	365.30	-722.60	0.00
Int + Body size	3	364.14	-722.30	0.33
Int + Gen. length	3	352.85	-699.70	22.90
Int	2	349.15	-694.30	28.30

Bill length rate

Model	K	logLik	AIC	ΔAIC
Int + Body size	3	282.93	-559.90	0.00
Int + Gen. length + Body size	4	283.43	-558.90	1.01
Int + Gen. length	3	273.70	-541.40	18.48
Int	2	271.19	-538.40	21.48

Wing length rate

Model	K	logLik	AIC	ΔAIC
Int + Body size	3	327.58	-649.20	0.00
Int + Gen length + Body size	4	328.22	-648.40	0.71
Int + Gen length	3	326.51	-647.00	2.14
Int	2	324.90	-645.80	3.36

Table S6. Relationships between rates of change in morphological traits and generation length and species' mean body size are robust to the inclusion of sample size. Rates of change in tarsus, bill, and wing lengths, and body mass were modeled as a function of log-transformed estimates of species generation length (Gen. length), log-transformed mean body size (Body size), and sample size (n). All models were run with simultaneous estimation of Pagels' λ. Sample size was never significantly associated with the rate of change in traits and controlling for sample size did not impact the effects of mean body size or generation length in any of the models.

Morphological Trait	Dataset	Variable	Coefficient	Standard Error	T-Value	P-Value
Tarsus length	Chicago	Intercept	-1.13E-03	1.28E-04	-8.80	< 0.001
		Gen. length	-3.21E-06	1.02E-04	-0.03	0.98
		Body size	1.85E-04	2.84E-05	6.53	< 0.001
		n	-9.10E-09	5.73E-09	-1.59	0.12
Bill length	Chicago	Intercept	-5.61E-03	7.70E-04	-7.28	< 0.001
		Gen. length	2.76E-04	6.27E-04	0.44	0.66
		Body size	9.27E-04	1.73E-04	5.38	< 0.001
		n	-1.20E-08	3.53E-08	-0.34	0.73
Wing length	Chicago	Intercept	5.99E-04	2.18E-04	2.74	0.01
		Gen. length	-1.57E-04	2.17E-04	-0.72	0.47
		Body size	-1.10E-04	5.44E-05	-2.03	0.05
		n	7.60E-09	1.26E-08	0.60	0.55
Body mass	Amazon	Intercept	-1.75E-03	1.10E-04	-15.99	< 0.001
		Body size	2.49E-04	3.27E-05	7.61	< 0.001
		n	-2.19E-08	1.04E-07	-0.21	0.83
Wing length	Amazon	Intercept	6.48E-04	8.94E-05	7.25	< 0.001
		Body size	-1.45E-04	2.36E-05	-6.15	< 0.001
		n	-1.74E-08	6.43E-08	-0.27	0.79
Wing length	Chicago & Amazon	Intercept	6.01E-04	9.33E-05	6.44	< 0.001
		Body size	-1.37E-04	2.21E-05	-6.21	< 0.001
		n	1.35E-08	1.03E-08	1.31	0.19

Table S7. The interaction between body size and migration phenology does not affect the relationship between morphological shifts and species' mean body size in the Chicago birds. The logarithms of tarsus, wing, and bill lengths were modeled as a function of year (transformed to start at 0), sex, age, and a three-way interaction between year, mean body size, and Julian day (Day) of the collection date for each specimen, with random intercepts and slopes for the effect of year for each species using linear mixed-effects models. Julian day was scaled to a mean of zero and a standard deviation of one to facilitate model convergence.

Morphological Trait	Variable	Estimate	Std. Error	t-value	P-value
Tarsus length	Intercept	2.37E+00	3.29E-02	72.22	<0.001
	Year	-1.24E-03	1.14E-04	-10.90	<0.001
	Sex(m)	1.87E-02	2.62E-04	71.24	<0.001
	Age (HY)	-3.82E-04	4.06E-04	-0.94	0.35
	Body size	2.67E-01	1.14E-02	23.42	<0.001
	Day	-2.69E-03	2.40E-03	-1.12	0.26
	Year * Body size	2.25E-04	3.95E-05	5.70	<0.001
	Year * Day	1.17E-04	8.74E-05	1.34	0.18
	Body size * Day	6.15E-04	8.04E-04	0.77	0.44
	Year * Body size * Day	-3.53E-05	2.93E-05	-1.21	0.23
Wing length	Intercept	3.38E+00	3.54E-02	95.56	<0.001
	Year	6.84E-04	1.25E-04	5.46	<0.001
	Sex(m)	4.88E-02	2.14E-04	227.64	<0.001
	Age (HY)	-1.36E-02	3.29E-04	-41.42	<0.001
	Body size	3.14E-01	1.23E-02	25.62	<0.001
	Day	8.15E-03	1.99E-03	4.09	<0.001
	Year * Body size	-1.29E-04	4.35E-05	-2.96	<0.01
	Year * Day	-1.14E-04	6.96E-05	-1.64	0.10
	Body size * Day	-1.16E-03	6.68E-04	-1.74	0.08
	Year * Body size * Day	3.76E-05	2.33E-05	1.61	0.11
Bill length	Intercept	1.25E+00	5.21E-02	24.02	<0.001
	Year	-5.59E-03	3.48E-04	-16.06	<0.001
	Sex(m)	1.53E-02	4.75E-04	32.30	<0.001
	Age (HY)	-1.75E-02	7.27E-04	-24.09	<0.001
	Body size	3.14E-01	1.81E-02	17.36	<0.001

Day	6.90E-03	4.48E-03	1.54	0.12
Year * Body size	8.43E-04	1.21E-04	6.94	<0.001
Year * Day	-5.07E-05	1.58E-04	-0.32	0.75
Body size * Day	-4.10E-03	1.50E-03	-2.73	0.01
Year * Body size * Day	5.95E-05	5.33E-05	1.12	0.26

Table S8. Phylogenetic uncertainty has minimal effects on PGLS model coefficients. We repeated our PGLS analyses using 100 randomly selected phylogenetic trees from the posterior distribution of the global phylogeny of birds (6) and calculated the means and standard deviations of the resulting coefficients. The mean coefficients were nearly identical to those generated with models that use a consensus tree (see Table S4). As in the models reported in Table S4, rates of change in tarsus, bill, and wing lengths were modeled as a function of log-transformed estimates of species generation length (Gen. length) and mean body size (Body size) for the Chicago dataset (Chi). For the Amazon dataset (Ama), rates of change in body mass and wing length were modeled as a function of log-transformed estimates of mean body size (Body size). Finally, rates of change in wing length of the Chicago and the Amazon datasets combined were modeled as a function of log-transformed estimates of mean body size (Body size). All models were run with simultaneous estimation of Pagels' λ.

Trait	Dataset	Variable	Mean Coefficient	Standard Deviation
Tarsus length	Chi	Gen. length	4.22E-05	3.43E-05
		Body size	1.82E-04	4.49E-06
Bill length	Chi	Gen. length	3.50E-04	9.57E-05
		Body size	8.96E-04	2.49E-05
Wing length	Chi	Gen. length	2.04E-04	1.40E-05
		Body size	9.96E-05	6.91E-06
Body mass	Ama	Body size	2.52E-04	1.41E-06
Wing length	Ama	Body size	1.43E-04	1.39E-06
Wing length	Chi & Ama	Body size	1.35E-04	2.21E-06

Table S9. The relationships between rates of change in morphological traits, generation length, and body mass are not related to census population size in the Chicago species. Rates of change in tarsus, bill, and wing lengths were modeled as a function of log-transformed estimates of species generation length (Gen. length), log-transformed species' mean body size (Body size) and population size (Pop. size) using our PGLS analyses. All models were run with simultaneous estimation of Pagels' λ. For population size estimates, we used the North American population size estimates from Partners in Flight (7) available for all 46 species.

Morphological Trait	Variable	Coefficient	Standard Error	T-Value	P-Value
Tarsus length	Intercept	-1.15E-03	1.29E-04	-8.89	<0.001
	Gen. length	3.10E-05	1.02E-04	0.30	0.76
	Body size	1.83E-04	2.91E-05	6.28	<0.001
	Pop. size	0.00E+00	0.00E+00	-0.50	0.62
Bill length	Intercept	-5.62E-03	7.79E-04	-7.22	<0.001
	Gen. length	3.22E-04	6.03E-04	0.53	0.60
	Body size	9.26E-04	1.74E-04	5.32	<0.001
	Pop. size	0.00E+00	0.00E+00	-0.41	0.69
Wing length	Intercept	5.99E-04	2.06E-04	2.91	0.01
	Gen. length	-1.39E-04	2.10E-04	-0.66	0.51
	Body size	-1.20E-04	5.30E-05	-2.27	0.03
	Pop. size	0.00E+00	0.00E+00	1.63	0.11

Table S10. Pearson's correlation coefficients (r) between the logarithm of species' mean body size and variance in log-transformed traits in the Chicago and Amazon datasets.

Morphological Trait	Dataset	r
Tarsus Length	Chicago	0.44
Wing Length	Chicago	0.02
Bill Length	Chicago	-0.10
Body Mass	Amazon	-0.19
Wing Length	Amazon	0.08

Methods S1. Why log transform morphological data?

In this study, we use linear regressions to estimate the rates of change of several morphological measurements through time in many species of different sizes. That is, we estimate the slope (change in measurement through time) knowing that each species has a different intercept (starting measurement value). This requires transformation of the morphological response variables because a regression predicting raw measurement values would estimate change expressed in measurement units through time, rather than percent change (change proportional to the starting value). Log-transformation (natural log) of raw measurements (the response variables) produces regression slopes that show percent rates of change (rather than change in measurement units). Mathematically, this is because changing a value by e.g., 1% changes the log of that value by approximately 0.01. Thus, we log-transformed our response variables prior to modeling. We show in the simulation below that failure to log transform (i.e., estimating change in raw units of measurement) could lead to the false conclusion that larger species are changing more through time, as they have a greater magnitude of change for a given % change due to their size, whereas log transformation allows accurate estimation of the percent change (rate of change).

```
Library(tidyverse)
library(lme4)
```

We start by imagining 10 species, ranging in body size from 5 to 50 grams. We call their starting average mass values “t1”, indicating mass in year 1.

```
T1 <- seq(5, 50, by = 5); t1

##  [1]  5 10 15 20 25 30 35 40 45 50

species <- paste(“species”, 1:length(t1)); species

##  [1] “species 1”  “species 2”  “species 3”  “species 4”  “species 5”
##  [6] “species 6”  “species 7”  “species 8”  “species 9”  “species 10”
```

Next, we generate normal distributions of 100 individuals for each species in year 1, centered around the mean starting (t1) value for that species. (We could instead use a log normal distribution). Then we replicate that distribution for each species 20 times (representing 20 consecutive time steps or years), but each year we reduce the measurement values by 5% (that is, every "species" experiences the same percent change in mass every year).

```
nyears = 20

sim.dat <- list()
for(i in 1:length(t1)){
  sim.dat[[i]] <- matrix(NA, 100, nyears)
  sim.dat[[i]][,1] <- rnorm(100, mean = t1[[i]]) ## normal distribution of 10
0 measurements, centered on the starting mean value for each species
  for(j in 2:nyears){
    sim.dat[[i]][,j] <- sim.dat[[i]][,(j-1)]*0.95 ## reduce measurements by 5
% for 19 more years
  }
  sim.dat[[i]] <- data.frame(cbind(sim.dat[[i]]))
  colnames(sim.dat[[i]]) <- paste0("year_", 1:nyears)
}

names(sim.dat) <- species

## convert list into dataframe
dat <- bind_rows(sim.dat, .id = "species") %>%
  pivot_longer(!species, names_to = "year_name", values_to = "mass") %>%
  mutate(year = rep(rep(1:nyears, 100),length(t1)))
```

Plot the data to visualize what's happening. First, we plot the changing distributions.

```
dat$species <- fct_reorder(dat$species, parse_number(dat$species))

dat %>%
  group_by(species, year) %>%
  ggplot(aes(year, mass)) +
  geom_point() +
  facet_wrap(~species)
```

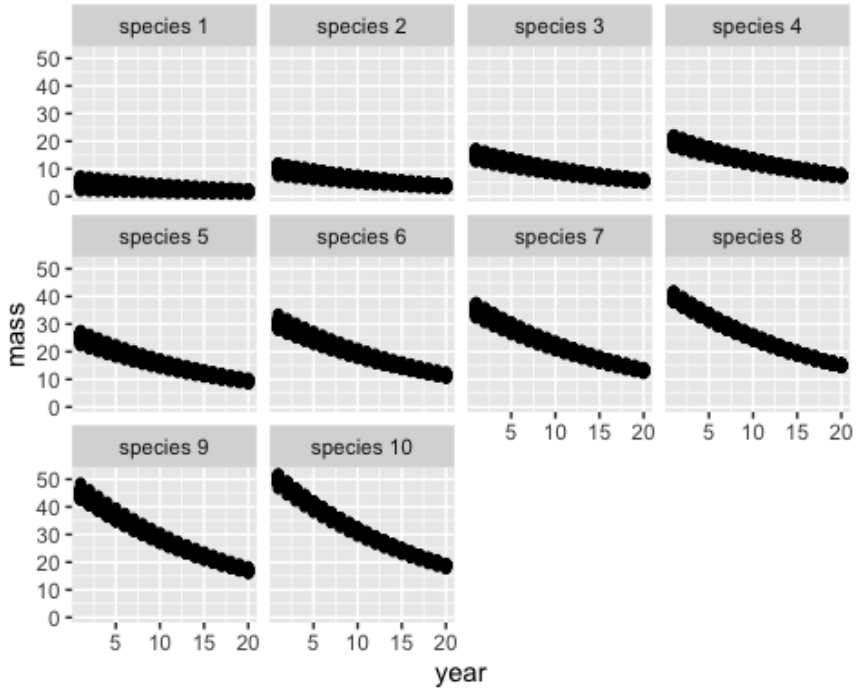

We can also plot the changing means:

```
dat %>%
  group_by(species, year) %>%
  summarize(mean_mass = mean(mass)) %>%
  ggplot(aes(year, mean_mass)) +
  geom_point() +
  facet_wrap(~species)
```

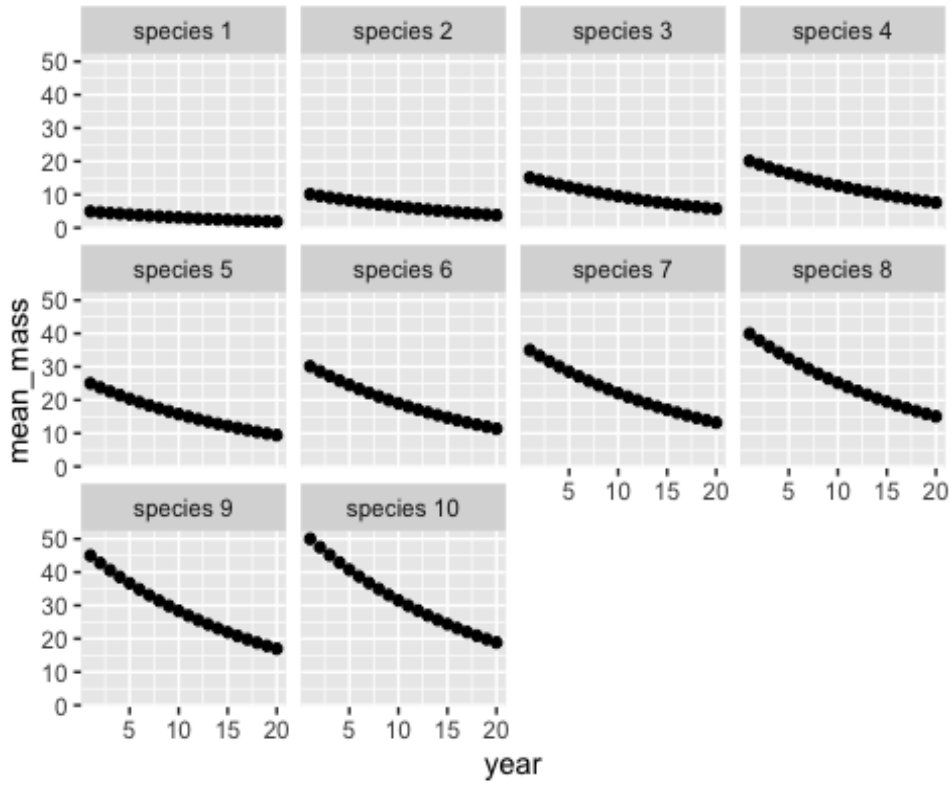

Note that species 1 through 10 get progressively "larger" (larger starting intercept value). In the plots above, it looks like the larger species are changing more, even though every species experienced a 5% change in measurement every year. We can show this apparent trend further by plotting the slopes (change through time) in every measurement. First, we show the slopes of the raw measurements (without log transformation).

```
dat %>%
  ggplot(aes(year, mass, group = species)) +
  geom_smooth(method = "lm", se = F)
```

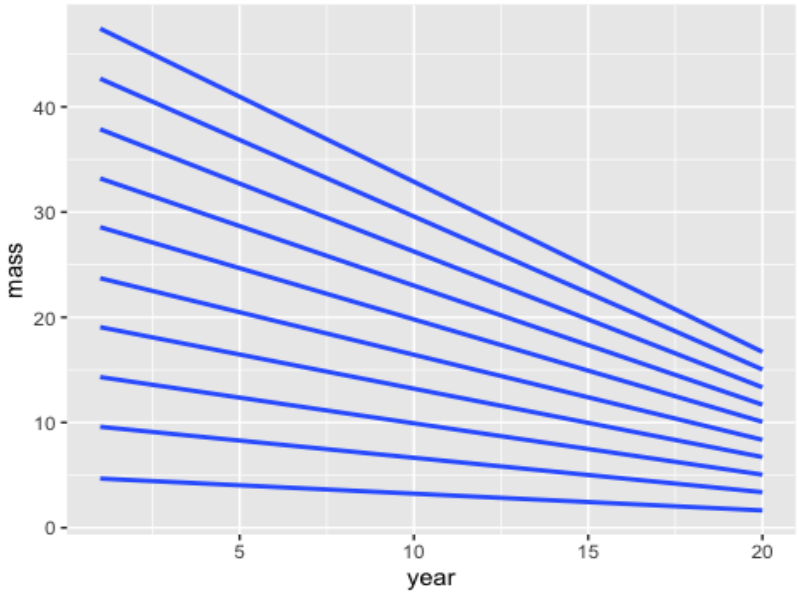

Again, in the above plot it looks like the larger species are changing more through time, but this is because the magnitude of the change is greater. By contrast, if we log transform the data, each slope becomes approximately the same and the slopes represent percent change (5% decrease for every species, in this case).

```
dat %>%
  ggplot(aes(year, log(mass), group = species)) +
  geom_smooth(method = "lm", se = F)
```

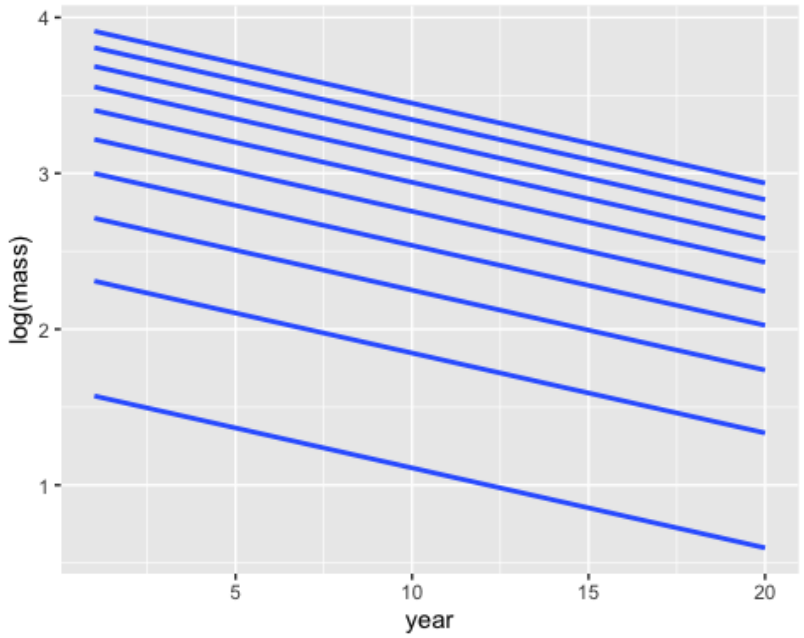

We can replicate the same phenomenon in a mixed modeling framework with random slopes for each species, which is the approach we take for analyzing the data in this paper. We produce a mixed model and use the random slope coefficients to represent percent change.

```
## mixed linear model without log transformation of "mass"
no_log_m<-lmer(mass~year + (1+ year|species), data=dat)

## mixed linear model with log transformation of "mass"
log_m<-lmer(log(mass)~year + (1+ year|species), data=dat)

## extract slope coefficients (we round them because there are very slight di
fferences)
rates_log_m <- round(coef(log_m)$species$year, 4)
rates_no_log_m <- round(coef(no_log_m)$species$year, 4)

## calculate species' mean mass across all years
means <- dat %>%
  group_by(species) %>%
  summarize(mean_mass = mean(mass))

## combine species mean mass with model rates
rates <- cbind(means, rates_no_log_m, rates_log_m)
```

The model with raw (not logged) mass indicates larger species change faster (they have more strongly negative slopes).

```
rates %>%
  ggplot(aes(mean_mass, rates_no_log_m)) +
  geom_point()+
  xlab("Species Mean Mass") +
  ylab("Slope Coefficients")
```

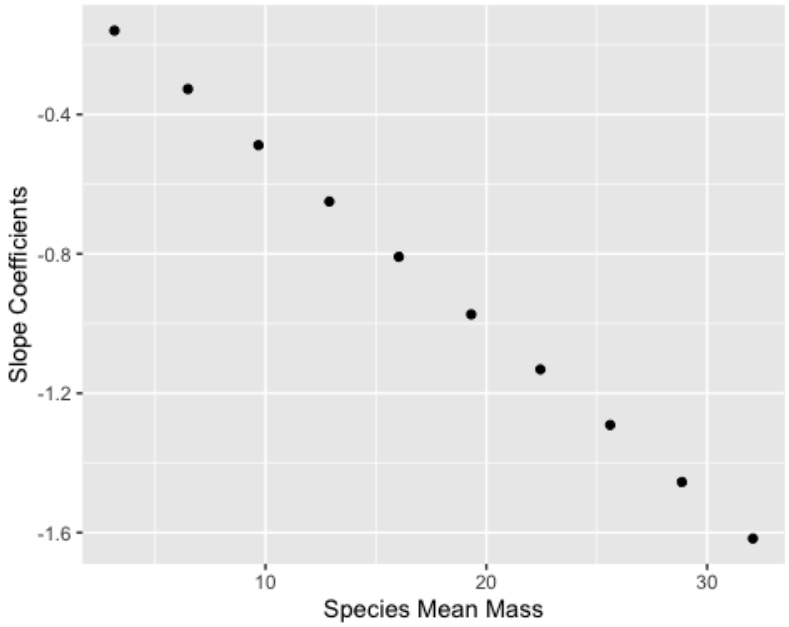

The model with log transformed mass has slope coefficients that are all approximately the same, representing the same percent change in mass for every species.

```
rates %>%
  ggplot(aes(mean_mass, rates_log_m)) +
  geom_point() +
  xlab("Species Mean Mass") +
  ylab("Slope Coefficients")
```

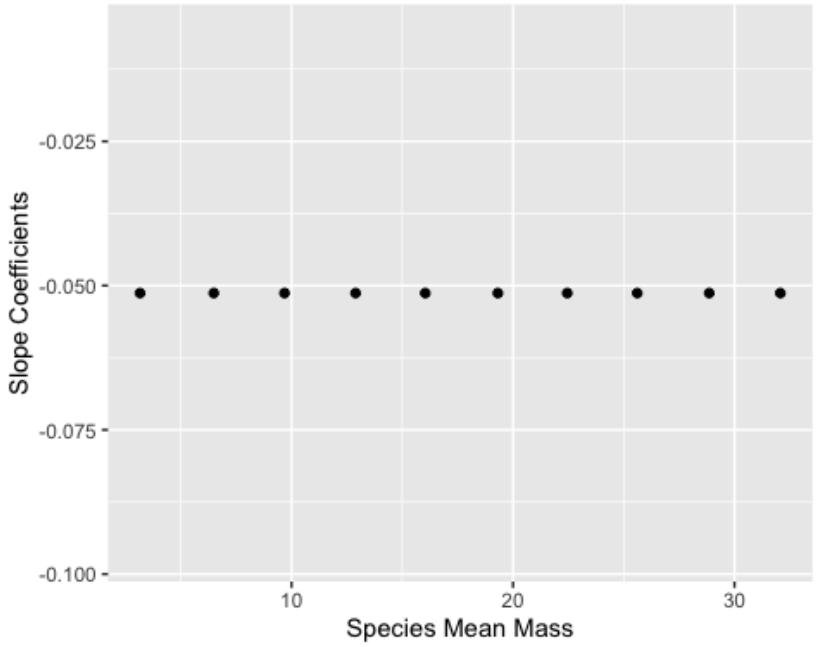

Therefore, log transformation allows us to accurately model the proportional change in a measurement, rather than the magnitude of the change.

Methods S2. Allometric scaling does not predict the observed relationship between species' mean body size and intraspecific rates of morphological change.

Body mass has allometric relationships with most morphological traits (1, 8–12). Specifically, larger individuals tend to have morphological characters such as tarsi, bills and wings that are relatively short for their body size compared to small individuals (13). Consequently, across taxa with varying body sizes, 1-dimensional traits (e.g., appendage lengths) vary at a constant rate that is a fraction of the rate of change in body size (3-dimensional volume or mass); this relationship often follows a 1/3 power law (1, 14). However, because this relationship is constant across body sizes, the same proportional decline in volume through time in a large versus a small bird should lead to the same proportional decline in tarsus length or bill length relative to body size (Fig. S8). That is, although smaller species have relatively longer appendages than larger species, this does not imply that their appendage length should shrink proportionately more when body size (volume) shrinks. Thus, the patterns we document are indicative of a faster rate of morphological change in small species than in large species that is not simply an artefactual outcome of allometric scaling.

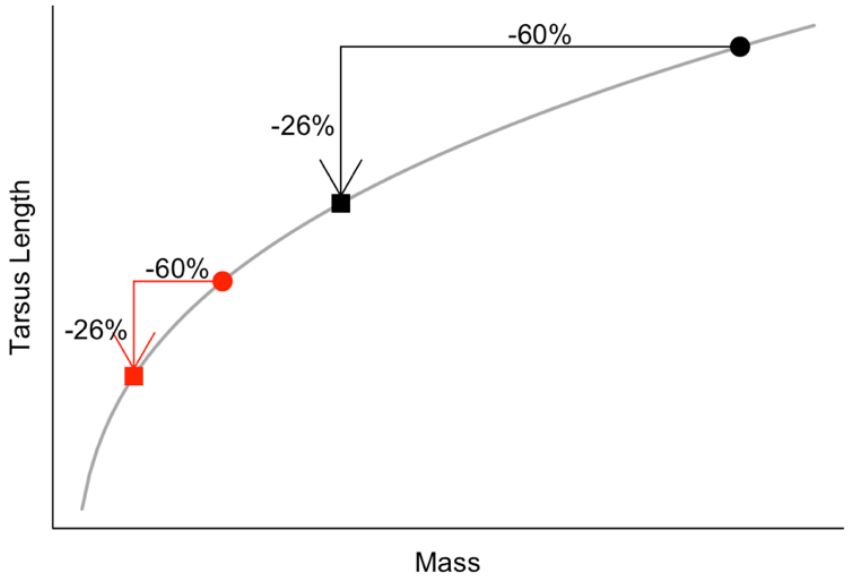

Figure S8. Equivalent reductions in percent body size (Mass) are expected to result in the same percent reduction in a length measurement. In our data, tarsus length approximates mass$^{1/3}$, as predicted by allometry. In a perfect mass$^{1/3}$ relationship (grey curve), a 60% reduction in body mass is predicted to result in a 26% reduction in tarsus length, despite the absolute value of these mass reductions differing depending on the initial mass of a species. This is shown for two species (red and black, moving from the circle symbols to the square symbols). Thus, if all species in our dataset were changing by the same proportional amount of body mass through time, then they would also be expected to change by the same proportional amount in measurements including tarsus, bill, and wing lengths, regardless of their mean body mass. Instead, we observed that smaller species are experiencing greater percent changes in tarsus, bill, and wing lengths than larger species.

Methods S3. Simulation examining the effects of potential error in generation length estimates on its relationship with rates of morphological change

Our estimates of species' mean body size are very precise as we have body mass measurements for all individuals in our study. For generation length (GL), however, estimates come from another published source (2), and it is difficult to estimate the uncertainty in these values. To better understand the consequences of potential error in the GL estimates, we conducted a simulation using the Chicago dataset. We ask, if rates of change in tarsus length (Δ tarsus) were in fact as highly correlated with GL as they are with mean body size (one of our strongest relationships; $r^2 = 0.705$), how much random error in GL estimates would it take to reduce the correlation to what we observe between rates of change in tarsus length and GL ($r^2 = 0.121$).

To do this, we first modified GL estimates for each species by the minimal amount necessary to achieve a correlation equivalent to the Δ tarsus ~ body size relationship ($r^2 = 0.705$). Specifically, we iteratively moved all estimates slightly closer to the best fit regression line, at a rate proportional to their residual values (1% of residual value per iteration), until we achieved an equivalent r^2 value for the Δ tarsus ~ GL relationship (original $r^2 = 0.121$, simulated $r^2 >= 0.705$). We used these simulated best-fit GL estimates in the next part of our simulation. Next, we introduced increasingly larger normally distributed random error to each of these best-fit GL estimates. The added error had a mean of zero and a standard deviation that started as 1% of the mean simulated best-fit estimated GL across species (0.019 years) and increased by an additional 1% per step. For each standard deviation level step, we ran 500 iterations to generate a confidence interval around mean estimates of r^2 values for each standard deviation level. We

then calculated the mean standard deviation of error that would be required to reduce the simulated r^2 value of 0.705 to that observed empirically in our dataset ($r^2 = 0.121$).

We found that introducing error into our simulated best-fit GL estimates with a mean of zero and a standard deviation of 0.271 years (95% CI: 0.136 – 0.873 years) was sufficient to reduce the r^2 values from 0.705 to 0.121 (Fig. S9). This indicates that adding values drawn randomly from the normal distribution $N(\mu = 0, sd = 0.271)$ to each best-fit simulated GL estimate resulted in an r^2 value equivalent to what we observe in our dataset using published GL estimates. Fig. S10a shows a histogram of the randomly generated absolute error values resulting from this distribution, in years (i.e., in absolute terms).

Finally, to think about how large errors would have to be in relative terms (% of GL by species), we calculated the median absolute error of standard deviation as a percent of best-fit GL estimates. To visualize what the median absolute error from the above distribution (median = 0.184 years) looks like across species in terms of % of species' simulated best-fit GL estimates, we divided the best-fit GL estimate for each species by that median value (Fig. S10b). This median absolute error is the equivalent of an absolute error that is 9.7% of the simulated best-fit generation length estimate of the median species and ranges from 8.1% to 10.9% across all species.

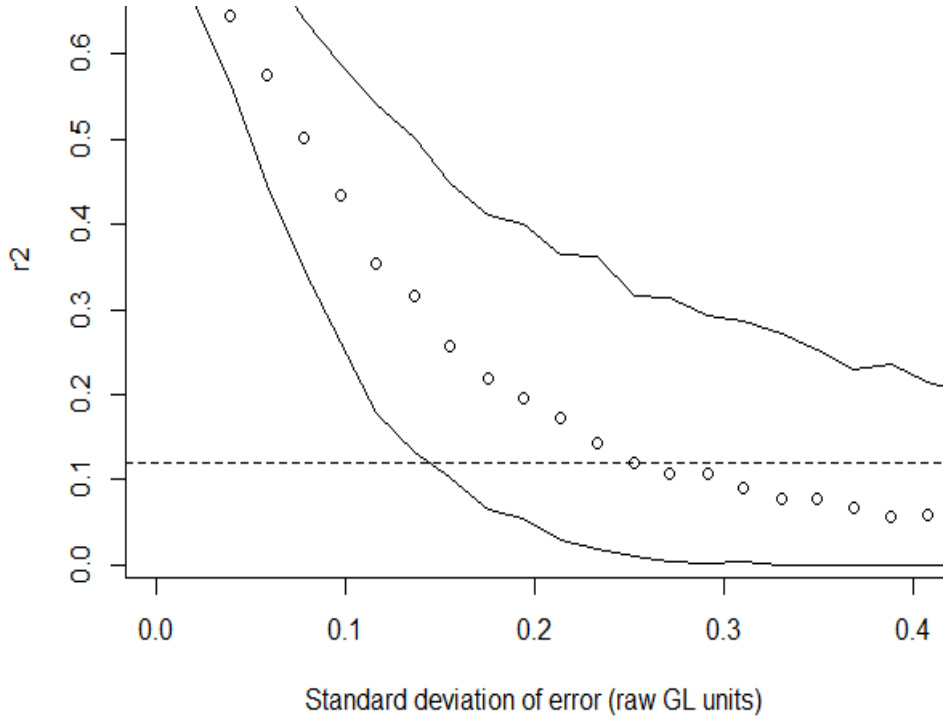

Figure S9. Relationship between the standard deviation of error in simulated best-fit generation length (GL) estimates and r^2 values in a Δ tarsus length ~ GL linear model. Dots show median of 500 iterations, and lines show 95% confidence interval. Horizontal dashed line indicates r^2 value of 0.121 (the relationship observed in our dataset).

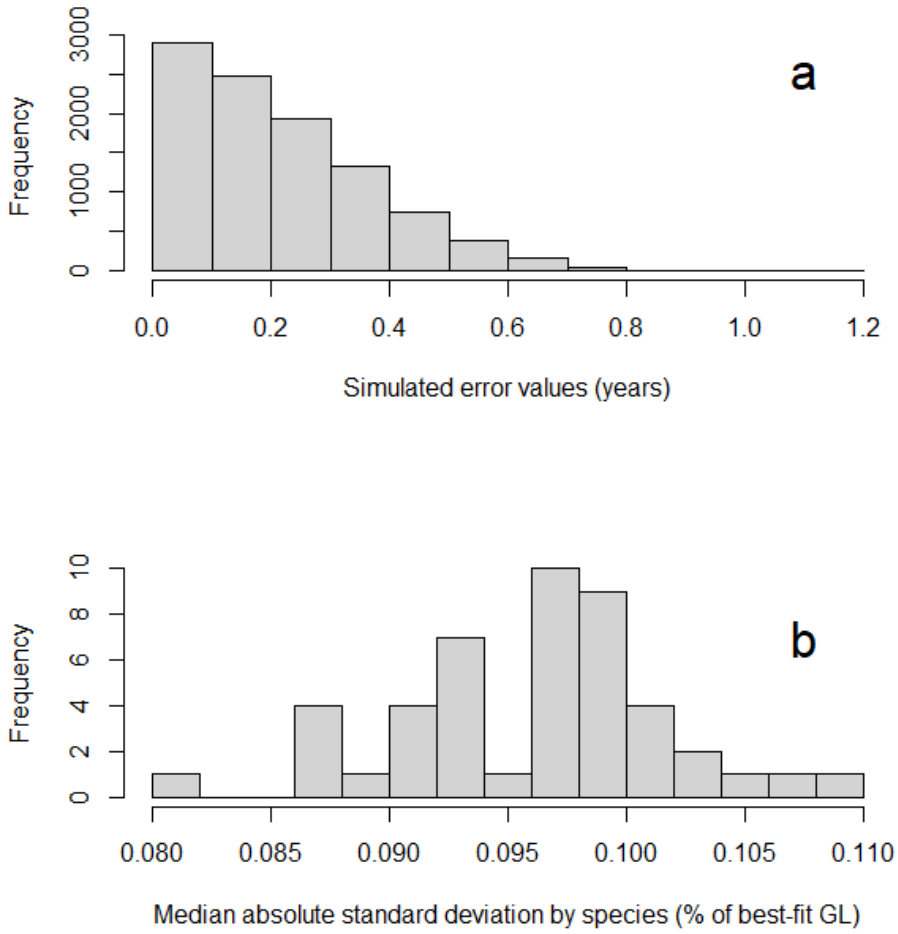

Figure S10. The median absolute error necessary to reduce model fit between Δ tarsus length and simulated best-fit generation length (GL) estimates to the value observed in our data. A) Distribution of raw absolute error values (in years). B) Distribution of the median absolute error value as a % of best-fit GL for each species.

SI REFERENCES

1. S. J. Gould, Allometry and size in ontogeny and phylogeny. *Biol. Rev.* **41**, 587–640 (1966).
2. J. P. Bird, *et al.*, Generation lengths of the world's birds and their implications for extinction risk. *Conserv. Biol.*, cobi.13486 (2020).
3. K. W. Chesser, R. T., S. M. Billerman, K. J. Burns, C. Cicero, J. L. Dunn, B. E. Hernández-Baños, A. W. Kratter, I. J. Lovette, N. A. Mason, P. C. Rasmussen, J. V. Remsen, Jr., D. F. Stotz, Check-list of North American Birds. *Am. Ornithol. Soc.* (2021).
4. K. J. Z. Remsen, J. V., Jr., J. I. Areta, E. Bonaccorso, S. Claramunt, A. Jaramillo, D. F. Lane, J. F. Pacheco, M. B. Robbins, F. G. Stiles, A classification of the bird species of South America. *Am. Ornithol. Soc.* (2022).
5. P. E. Johnson, Rockchalk: Regression estimation and presentation. *Available https//cran.r-project.org/package=rockchalk, Accessed 23rd Nov 2021*.
6. W. Jetz, G. H. Thomas, J. B. Joy, K. Hartmann, A. O. Mooers, The global diversity of birds in space and time. *Nature* **491**, 444–448 (2012).
7. Partners in Flight, Population Estimates Database, version 3.1. *Available at http://pif.birdconservancy.org/PopEst* (2020).
8. K. Schmidt-Nielsen, Scaling in biology: The consequences of size. *J. Exp. Zool.* **194**, 287–307 (1975).
9. J. S. Huxley, Constant differential growth-ratios and their significance. *Nature* **114**, 895–896 (1924).
10. C. P. Klingenberg, Heterochrony and allometry: The analysis of evolutionary change in ontogeny. *Biol. Rev.* **73**, 79–123 (1998).
11. R. C. Stillwell, A. W. Shingleton, I. Dworkin, W. A. Frankino, Tipping the scales:

Evolution of the allometric slope independent of average trait size. *Evolution* **70**, 433–444 (2016).

12. C. Pélabon, *et al.*, Evolution of morphological allometry. *Ann. N. Y. Acad. Sci.* **1320**, 58–75 (2014).

13. J. A. Bright, J. Marugán-Lobón, S. N. Cobb, E. J. Rayfield, The shapes of bird beaks are highly controlled by nondietary factors. *Proc. Natl. Acad. Sci. U. S. A.* **113**, 5352–5357 (2016).

14. G. G. Simpson, *Tempo and Mode in Evolution.* (Columbia University Press, 1944).